Chen, H, Huang, S, Niu, D, Gao, Y and Zhang, Z

Fatigue characterization and assessment methods for the terminal blend crumb rubber/SBS composite modified asphalt binders

Fatigue characterization and assessment methods for the terminal blend crumb rubber/SBS composite modified asphalt binders

Huikun Chen [a], Shan Huang [a], Dongyu Niu [a,*], Yangming Gao [b], Zhao Zhang [a]

a School of Materials Science and Engineering, Chang'an University, Xi'an, 710061, China.

b School of Civil Engineering and Built Environment, Liverpool John Moores University, Byrom Street, L3 3AF, Liverpool, United Kingdom.

Abstract: In this study, we investigated the fatigue performance of SBS/terminal blend crumb rubber (TB) composite modified asphalt binder to extend the service life of pavements. Six types of modified asphalt binders were prepared and subjected to Time Sweep (TS) and Linear Amplitude Sweep (LAS) tests to analyze fatigue damage and fatigue life. Utilizing the Taylor diagram and Threat Score (T_S) method, we aimed to optimize fatigue damage evaluation models and indicators suitable for SBS/TB composite modified asphalt binder. The results demonstrate a significant improvement in the fatigue resistance of asphalt binders at low and high strain levels with the SBS/TB composite modifier. Analysis of the Taylor diagram and TS results revealed that the 20% DER deviation criterion and viscoelastic continuum damage (VECD) models yield similar simulation effects on DSR-C calculated fatigue life results. These models exhibit better performance in terms of standard deviation and root mean square error (RMSE), albeit with a slightly lower correlation coefficient. Conversely, the 50% G* criterion model demonstrates an excellent fitting effect on the correlation coefficient (Sample Correlation Coefficient, R=0.9289), albeit with significant standard deviation and RMSE. The S×N peak criterion model shows a better fit for the correlation coefficient while displaying a weaker fit with the standard deviation. Ultimately, we propose the DSR-C model, 20% DER deviation criterion, and VECD model as more suitable fatigue damage evaluation models for SBS/TB composite modified asphalt binder. This study underscores the significance of these findings and their alignment with similar investigations, suggesting avenues for further improvement and research in the field.

Keywords: Terminal blend crumb rubber (TB), SBS, Modified asphalt binder, Fatigue damage, Assessment methods

1 Introduction

According to a report by the Tire Industry Project for the World Business Council for Sustainable Development, 1 billion end-of-life tires are generated every year and there are currently 4 billion such tires in landfills and stockpiles worldwide. Waste tires, as recyclable high-polymer materials, have garnered worldwide attention for their potential for recycling and reuse. In recent years, converting waste tires into rubber powder modifiers and incorporating them into asphalt pavement has been recognized as a green solution[1]. This modification method can significantly consume waste tires, reducing reliance on natural resources in road construction. Terminal blend rubberized asphalt (TBRA) has gradually gained the attention of researchers due to its excellent storage stability and favorable construction properties[2, 3].

Given the promising prospects of TBRA, numerous scholars have conducted research on it. Many have found that TBRA exhibits good fatigue resistance, deformation resistance, and performs well in low temperatures but lacks in high-temperature performance. Presently, many researchers are blending SBS with TB to enhance high-temperature performance of modified asphalt. TB, as a rubber based modifier, can improve toughness and tear resistance of asphalt binder, further enhancing its fatigue performance[4]. On the other hand, SBS is a thermoplastic elastomer that undergoes phase changes at high temperatures, increasing the asphalt binder elasticity and thus reducing fatigue damage.

Currently, some scholars have researched fatigue performance of SBS/TB composite modified asphalt binder[5]. To evaluate fatigue performance of SBS/TB composite modified asphalt binder, researchers often employ fatigue testing methods. These tests include strain-controlled tests, stress-controlled tests, and repeated loading tests, simulating the loads that asphalt undergoes in real-world usage, allowing an accurate assessment of its fatigue performance[6]. Fatigue cracking is a major distress caused by repeated traffic loading during the long-term service life of asphalt pavements, and the fatigue resistance of asphalt pavement mainly depends on the rheological and adhesive properties of the asphalt binder in the mixture[7, 8]. Therefore, accurately characterizing and quantifying asphalt binder fatigue resistance has been a core issue in research for the past few decades.

Numerous testing methods and evaluation parameters have been proposed for assessing fatigue resistance of asphalt binders. In the Strategic Highway Research Program (SHRP) in the United States, a fatigue parameter ($|G^*|\cdot\sin\delta$) was introduced for evaluating the asphalt binder fatigue performance at intermediate temperatures. However, it was found that SHRP fatigue parameters had a limited correlation with the fatigue life of asphalt mixtures and pavements[9-11]. Because G^* and δ are obtained within the linear viscoelastic region of the asphalt binder, without considering damage effects. Polymer modified asphalt binder, in particular, can withstand higher strains before cracking, and thus, better methods for evaluating its fatigue resistance were sought.

The National Cooperative Highway Research Program (NCHRP) Project 9-10 introduced Time Sweep (TS) repeated cyclic loading tests to study asphalt binder fatigue performance[12]. TS tests have been widely used to determine asphalt binder fatigue failure criteria[13-15]. Based on TS testing data, researchers have proposed a series of fatigue damage evaluation parameters. Although such representative evaluation parameters can easily assess the fatigue damage of asphalt binders, they are empirical and do not quantitatively describe the fatigue damage state of asphalt binder under cyclic loading. Consequently, subsequent research work has tended to use energy concepts as an alternative definition of fatigue failure and has applied the dissipated energy ratio (DER)[13, 14, 16] and rate of dissipated energy change (RDEC)[17-19] widely in asphalt binder fatigue analysis. DER parameters have been shown to have a good correlation with pavement fatigue testing, but their definition of asphalt

binder fatigue damage is indirect to some extent and still falls into the category of empirical indicators. Moreover, the testing time is often long and cumbersome.

Given the limitations of TS testing, the American Association of State Highway and Transportation Officials (AASHTO) developed an accelerated fatigue procedure known as the Linear Amplitude Sweep (LAS) test (AASHTO-TP101). This test is conducted at constant temperature and frequency, gradually increasing strain amplitudes to measure the fatigue damage limit of asphalt binder[20, 21]. Although the LAS test significantly reduces the testing duration and provides preliminary insights into asphalt binder fatigue behavior, it may cause cracking due to excessive loads as the strain amplitudes gradually increase, rather than fatigue cracking caused by repeated loading. Furthermore, LAS testing involves formula calculations and parameter fitting, which can be cumbersome and somewhat empirical. Therefore, the VECD model, which attempts to clarify the fatigue damage mechanism of asphalt binder, remains inconclusive. The parameters or models used to evaluate asphalt binder fatigue damage as described above are often empirical or semi-empirical and lack intuitiveness.

Further investigation is required to delve into the fatigue damage mechanism of asphalt binder from a fundamental mechanical perspective, particularly concerning crack propagation under rotational shear forces. Additionally, a direct assessment of asphalt binder fatigue crack resistance could be achieved by predicting crack propagation based on crack length in asphalt binder. Several studies have already initiated direct investigations into crack growth in asphalt binder. For instance, Hintz and Bahia[22] utilized DSR Time Sweep (TS) testing and digital visualization to observe crack growth trends in asphalt binder samples. Shan, Tian, He, and Ren[23] employed experimental and image analysis methods to determine internal crack propagation in asphalt binder samples subjected to shear fatigue. The research shows that under the action of rotational shear fatigue loads, fatigue cracks in asphalt binder specimens are "edge cracks" that initiate from the outer periphery and propagate inward, producing a rough fracture surface with radial peaks and valleys. Circumferential cracks reduce the effective radius of cylindrical samples, and the effective radius has a good correlation with the degree of fatigue damage in asphalt binder, serving as a new evaluation indicator.

SBS/TB composite modified asphalt binders have been widely used, but it is currently unclear which model can better characterize the fatigue performance of SBS/TB composite modified asphalt binder. while assessment parameters or models for fatigue performance have often been empirical or semi-empirical, further research is needed to understand the fatigue damage mechanisms of asphalt binder from the perspective of crack propagation.

In this study, this paper aims to use TS test criteria, VECD model, and DSR-C model to compare and study the fatigue damage behavior of SBS/TB composite modified asphalt binder. The applicability and accuracy of the relevant models are verified using the actual failure morphology images of asphalt binder after fatigue testing. On this basis, Taylor plot analysis method is used to compare and analyze the simulation accuracy of various fatigue damage evaluation models, and select a fatigue damage evaluation model that is more suitable for SBS/TB composite modified asphalt binder.

2 Materials and Experimental Methods

2.1 Materials

In this study, the base asphalt binder used was SK70# road petroleum asphalt binder, and its basic technical specifications are listed in Table 1. The linear SBS polymer matrix for preparing the composite modified asphalt binder was T161B produced by Dushanzi Petrochemical Company in Xinjiang, China,

with a block ratio of 30:70. Its basic technical parameters are presented in Table 2. Rubber particles with a particle size of 80 mesh were used, and their main technical specifications are shown in Table 3.

Table 1 SK70# Road Petroleum Asphalt Technical parameters

Test		Values	Standard requirements	Testing method
Penetration at 25 °/mm		67	60~80	T 0604-2011
Softening point / ℃		52.5	≥46	T 0606-2011
Ductility at 15 °C		>100	≥100	T 0605-2011
Density at 15 °C /(g·cm^{-3})		1.037	Record of actual measurements	T 0603-2011
Viscosity at 135 ℃/(Pa·s)		2.608	≤3	T 0619-2011
Thin film oven test (TFOT)	Quality loss /%	-0.504	-0.8 ~ 0.8	T 0610-2011
	Penetration ratio /%	72	≥61	T 0604-2011
	Residual ductility at 15 ℃/cm	20	≥15	T 0605-2011

Table 2 T161B Linear SBS Technical Parameters

Technical Item	Test Result	Unit
Oil Content	0	Wt/%
Styrene Content	31	Wt/%
Volatile Content	0.38	Wt/%
300% Tensile Stress	2.41	MPa
Tensile Strength	25.4	MPa
Elongation at Break	750	%
Shore Hardness	79	Shore A

Table 3 Crumb rubber Basic Technical Parameters

Technical Item	Test Result	Technical Requirements
Relative Density	1.18	/
Heating Loss	0.38 %	≤1.0 %
Acetone Extractables	7 %	≤14 %
Carbon Black Content	30 %	≥28 %
Rubber Hydrocarbon Content	56%	≥48 %
Fiber Content	0.02 %	≤0.5 %
Metal Content	0.01 %	≤0.03 %

2.2 Preparation of Modified Asphalt Binder Samples

To ensure the uniform and stable preparation of the modified binder, a wet process known as Terminal Blend technology was employed to achieve desulfurization or dispersion of rubber in hot asphalt binder, ensuring its thorough dispersion. The specific preparation process is as follows:

a. Heat the SK70# base asphalt binder to approximately 200°C.

b. Add the designed amount of crumb rubber to the heated base asphalt binder.

c. Raise the temperature rapidly to 220°C and perform high-speed shearing at 220°C for 40-60 minutes with a rotation speed of 5000 rpm.

d. Gradually lower the temperature to 175°C.

e. Add the SBS modifier and maintain a constant rotation speed while continuing high-speed shearing for 1 hour.

f. Add a sulfur stabilizer at a mass fraction of 0.15% of the base asphalt and shear for 20 minutes.

g. Finally, place the mixture in a 165°C oven for 30 minutes for development.

h. Stir regularly during development to prevent separation.

The abbreviated names of the samples for various proportions are explained in Table 4.

Table 4 Abbreviations of Samples

Sample Name	Description
S_2	2% SBS Modified Asphalt binder
S_3	3% SBS Modified Asphalt binder
S_2R_{10}	2% SBS and 10% Rubber Composite Modified Asphalt binder
S_2R_{15}	2% SBS and 15% Rubber Composite Modified Asphalt binder
S_3R_{10}	3% SBS and 10% Rubber Composite Modified Asphalt binder
S_3R_{15}	3% SBS and 15% Rubber Composite Modified Asphalt binder

2.3 Time Sweep Test

The time sweep test is a strain-controlled fatigue assessment conducted at room temperature, aimed at ensuring the fatigue failure of asphalt binder by subjecting it to cyclic loading at low strain levels. The test utilizes parallel loading plates with an 8 mm diameter (with a 2 mm gap). Samples undergo 54,000 loading cycles at a temperature of 20°C, a frequency of 10 Hz, and a strain amplitude of 5%. This procedure helps in determining various parameters including the complex shear modulus, phase angle, and other fatigue characteristics of the samples under failure conditions.

From the gathered data, a range of fatigue failure criteria were employed to predict and evaluate the fatigue life of each sample. Among the multitude of available criteria, this study selected the most pertinent ones such as the complex modulus decay criteria, phase angle peak criteria, S×N peak criteria, and 20% DER deviation criteria. These criteria were utilized to assess the fatigue resistance performance of the modified asphalt binder.

2.4 Linear Amplitude Sweep Test (LAS)

According to AASHTO TP101, the LAS test was employed to assess the fatigue characteristics of SBS/TB modified asphalt binder. All LAS test specimens underwent 20 hours of aging using the PAV aging method. The testing temperature was maintained at 25°C, with samples having an 8 mm diameter and a parallel plate spacing of 2 mm. As a part of the accelerated program, the LAS test expedited the determination of parameters A and B in the conventional strain-controlled fatigue equation. These parameters are defined as follows:

$$N_f = A \cdot (\gamma_p)^{-B} \quad (1)$$

Where N_f represents the fatigue life. γ_p represents the applied shear strain amplitude.

The LAS test procedure comprises two main stages. Firstly, a constant shear strain amplitude of 0.1% was applied to the sample during a frequency sweep ranging from 0.2 Hz to 30 Hz. This initial stage aimed to capture the rheological properties of the samples within the Linear Viscoelastic (LVE) region without inducing damage. Secondly, an amplitude sweep was conducted to assess the damage characteristics of the samples. During this phase, the oscillating shear strain was incrementally increased from 0 to 30% over 5 minutes at a loading frequency of 10 Hz.

The parameters A and B in Equation (1) can be calculated using the viscoelastic material damage evolution mechanics model (S-VECD model) from the VECD theory[24]. The formula for calculating the fatigue parameters in this model is as follows:

$$D(t) = \sum_{i=1}^{N} [\pi \gamma_0^{\,2} (C_{i-1} - C_i)]^{\frac{\alpha}{1+\alpha}} (t_i - t_{i-1})^{\frac{1}{1+\alpha}} \quad (2)$$

$$C(t) = C_0 - C_1 (D)^{C_2} \quad (3)$$

$$D_f = \left(\frac{C_0 - C@PeakStress}{C_1}\right)^{1/C_2} \quad (4)$$

$$A = \frac{f \cdot (D_f)^{1+\alpha(1-C_2)}}{[1+\alpha(1-C_2)] \cdot (\pi C_1 C_2)^{\alpha}}; B = 2\alpha \quad (5)$$

Where D represents damage density. γ_0 represents the applied strain during the test. t is the test time. α is the reciprocal of the slope of the storage modulus G'_0 with respect to the logarithm of angular frequency, calculated from frequency sweep data. C(t) represents the ratio of the complex modulus of the sample at time t to the initial complex modulus, indicating material integrity. C_0 is the initial value of C, equal to 1. C@PeakStress is the material integrity value corresponding to the peak stress. C_1 and C_2 are curve-fitting parameters. D_f represents the fatigue failure criterion. f is the test loading frequency.

3 Results and Discussion

3.1 Time Sweep Test Results Analysis

3.1.1 Complex Modulus Decay Criterion

The 50% modulus decay criterion uses the number of loading cycles required for the specimen modulus to decrease by 50% as the fatigue life of the asphalt binder. To facilitate visual analysis, the normalized modulus ratio *S* was used as the research indicator. The relationship curves between *S* values and the number of loading cycles for various modified samples, as well as the predicted fatigue life results, are shown in Figure 1 and Figure 2, respectively.

From the results in the figures, it can be observed that at a 5% strain level, modified asphalt binders with high levels of SBS and TB content (S_2R_{15}, S_3R_{10}, S_3R_{15}) exhibit excellent fatigue resistance. Their normalized modulus ratios only decrease to 0.5 after 33,780, 41,820, and 60,180 cycles of oscillatory loading, respectively. Furthermore, it can be seen from the figures that the samples initially display a brief plateau region at the beginning of loading, followed by a sharp decline. This indicates that the addition of TB delays the fatigue damage initiation point in the SBS asphalt binder matrix. Based on Figure 2, the fatigue life ranking of the various samples according to the modulus decay criterion is as follows: $S_3R_{15} > S_3R_{10} > S_2R_{15} > S_3 > S_2R_{10} > S_2$.

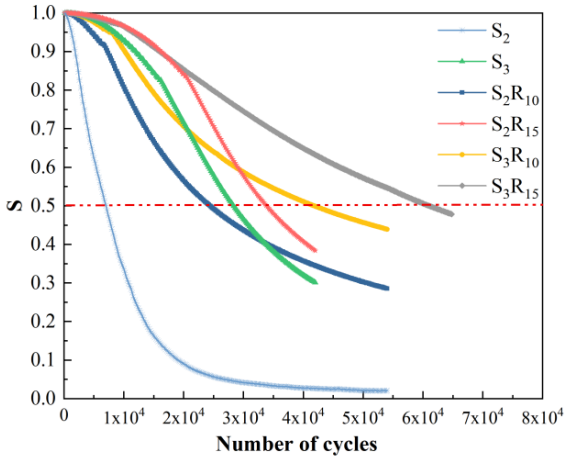

Figure. 1. Plot of Normalized Modulus versus loading cycles

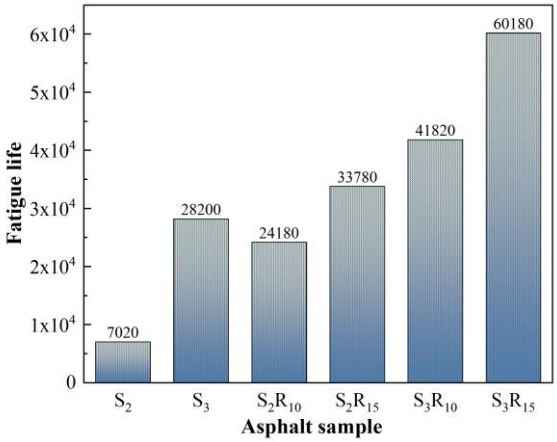

Figure. 2. Fatigue Life of Modified Asphalt Binders Based on Complex Modulus Decay Criterion

3.1.2 Phase Angle Peak Criterion

The phase angle peak is a phenomenological indicator. Fatigue life is defined as the number of loading cycles at which the asphalt binder reaches its highest phase angle value. The variation of phase angle with the number of loading cycles for each sample obtained from the time sweep test is shown in Figure 3. From the results in the figure, it can be observed that the phase angles of S_2 and S_3 show an anomalous increase, which may be due to the low polymer concentration, causing the binder to exhibit shear thinning behavior. On the other hand, the phase angle peak values of S_2R_{10}, S_2R_{15}, S_3R_{10}, and S_3R_{15} occur at around 1000 loading cycles with little difference. Therefore, the fatigue life determined based on the phase angle peak criterion is not reliable[25]. Due to the unclear theoretical background of phase angle peaks, this method is considered unsuitable for evaluating the fatigue resistance of SBS/TB composite modified asphalt binder in this study.

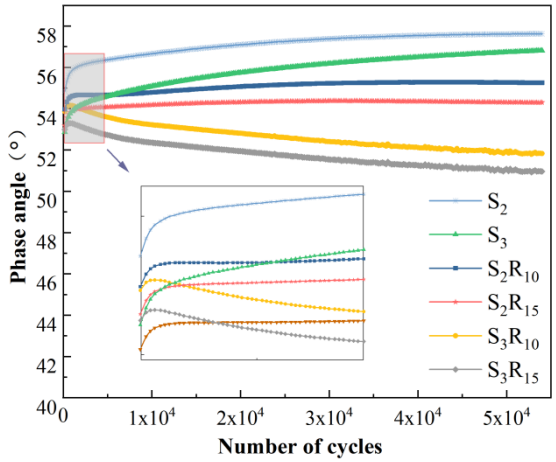

Figure. 3. Plot of Phase Angle versus loading cycles

3.1.3 S×N Peak Criterion

The S×N peak is a phenomenological indicator, where *S* represents the normalized modulus ratio defined during the fatigue test period, and *N* is the number of loading cycles. Fatigue life is defined as the number of loading cycles at which the asphalt binder reaches its highest *S*×*N* value. According to the results in Figure 4, it can be observed that only S_2, S_3, S_2R_{10}, and S_2R_{15} exhibit peaks. Among them, S_2 shows the earliest peak, and an increase in the amounts of SBS and TB both leads to an increase in the *S*×*N* values of the samples, with the peaks showing a significant delay. However, when the SBS

content reaches 3%, it can be seen that no peaks appear in the two samples, indicating that S_3R_{10} and S_3R_{15} have better fatigue resistance. In general, the fatigue life of each sample determined based on the S×N peak criterion is highly consistent with the results obtained from the complex modulus decay criterion.

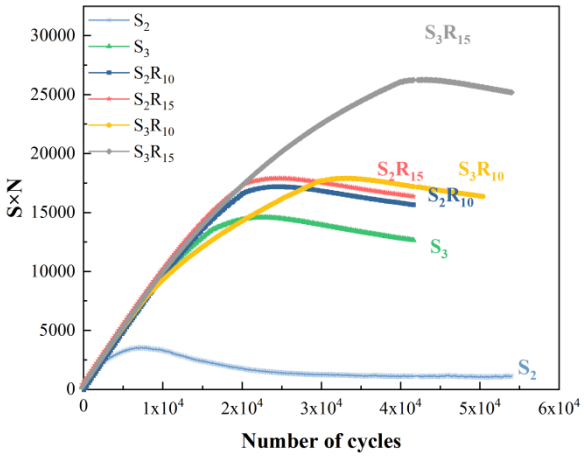

Figure. 4. Plot of S ×N versus loading cycles

3.1.4 20% DER Deviation Criterion

The 20% DER deviation is an energy energy-based criterion. The energy dissipation (W_i) during each loading cycle is calculated using equation (6). By summing up the energies for each cycle, cumulative energy dissipation up to a target loading cycle n is quantified. Correspondingly, DER is defined as the ratio of cumulative energy dissipation up to loading cycle n to the energy dissipation at loading cycle n[14], as shown in equation (7).

$$W_i = \pi \sigma_i \varepsilon_i \sin\delta_i \quad (6)$$

$$DER = \frac{\sum_{i=1}^{n} W_i}{W_n} \quad (7)$$

Where W_i represents the energy dissipation at loading cycle i, σ_i is the stress amplitude at loading cycle i, ε_i is the strain amplitude at loading cycle i, δ_i is the phase angle corresponding to loading cycle i, $\sum_{i=1}^{n} W_i$ represents the sum of total energy dissipation up to loading cycle n, and W_n represents the energy dissipation at loading cycle n. According to Bonnetti research, asphalt binder fatigue life is defined as the number of loading cycles where DER deviates 20% from the undamaged linear line[26]. Each asphalt binder was tested at least three times to obtain an average value, with a coefficient of variation of less than 15%.

The DER test results for each sample are shown in Figure 5. At a 5% strain level, when the number of loading cycles is less than 10,000, all modified asphalt binders have DER deviation values less than 20%, indicating that the modified asphalt binders have not yet undergone fatigue damage. With an increase in the number of cycles, the DER curves of the various samples begin to show significant differences. According to the 20% DER deviation criterion, it can be seen that both SBS and TB have an improving effect on the fatigue resistance of asphalt binder, and the influence pattern is consistent with the complex modulus decay results. Furthermore, based on the calculation method of DER, it can be deduced that under a fixed strain level, the evolution of DER is mainly dominated by the changes in

G^* and phase angle. Combining the changes in G^* and phase angle (Figures 1 and 2), it can be concluded that G^* has a greater impact on DER decay. For example, in the case of S_2, at the loading cycle where its DER deviates by 20%, its complex modulus has decayed by 57%, while the phase angle has changed only by 4.5%. Thus, it can be inferred that the fatigue life determined by both the modulus decay criterion and the 20% DER deviation criterion is highly correlated.

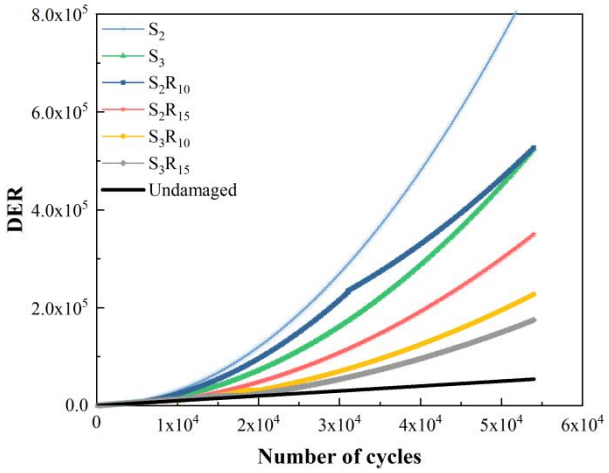

Figure. 5. Plot of DER versus loading cycles

3.2 LAS Analysis

The results of LAS tests and the fatigue parameters calculated by the S-VECD model for each sample are presented in Table 5, and the relationship curves for these parameters are shown in Figures 6 to 8.

Figure 5 LAS testing fatigue parameter results based on S-VECD model

Asphalt binder	α	C_1	C2	A(×105)	B
S_2	1.392	0.052	0.514	2.002	-2.785
S_3	1.394	0.051	0.485	6.979	-2.789
S_2R_{10}	1.279	0.031	0.570	3.087	-2.557
S_2R_{15}	1.489	0.068	0.432	15.663	-2.978
S_3R_{10}	1.493	0.070	0.429	18.586	-2.987
S_3R_{15}	1.615	0.091	0.382	70.772	-3.229

Figure 6 presents the stress-strain curve results for PAV samples with different dosages of modifiers. It can be observed that as the shear strain increases, the shear stress response of the seven asphalt binders reaches a peak at a certain point, which is the yield stress of the asphalt material, corresponding to the yield strain[27]. After the peak, the shear stress rapidly decreases, indicating severe damage to the material at this point. During this process, it can be noted that the peak values and their corresponding widths vary among different samples. Among them, S_2 and S_3 have narrower peak widths, while the addition of TB significantly widens the yield stress peak, and the widening effect of the peak width is usually attributed to the increase in the percentage of large molecular substances[28]. This suggests that SBS/TB composite modified asphalt binder exhibits less strain dependence and better fatigue resistance due to the increased content of large molecular polymers. Regarding the stress peak values for each curve, it can be seen from the graph that S_2 and S_3 have higher yield stress values, indicating that single SBS modified asphalt binder lacks ductility and is more prone to brittle fracture. The addition of TB,

on the other hand, helps reduce the stress peak values. This may be because during the amplitude scanning process, SBS and TB do not form an appropriate network in the asphalt binder, indicating that TB can increase the toughness of the asphalt binder.

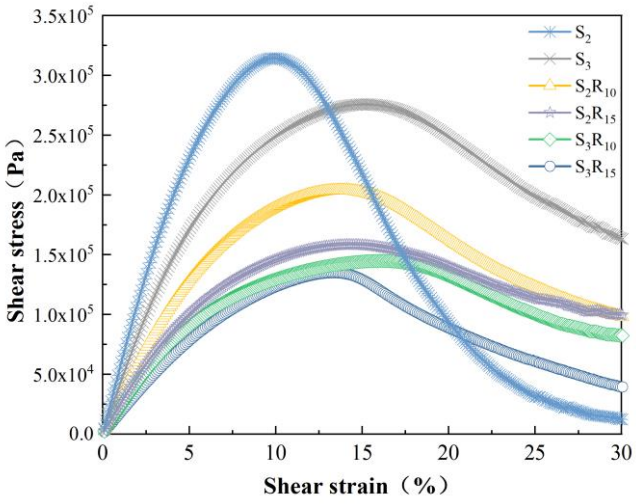

Figure. 6. Stress-Strain Curves for Various Samples

The S-VECD model can quantify the relationship between damage density (*D*) and material integrity (C), as shown in Figure 7. With damage density kept constant, higher *C* values represent better material integrity, indicating that the asphalt binder can withstand more load cycles and exhibit better durability, i.e., improved fatigue performance[29]. From the curves, it can be seen that SBS/TB composite modified asphalt binder has higher *C* values at lower damage densities, indicating superior fatigue resistance compared to S_2 and S_3. As damage density increases, there is no significant difference in *C* values for different dosages of SBS/TB modified asphalt binders, and the improvement in durability compared to single SBS modified asphalt binder is not significant. Comparing various composite modified asphalt binders, it can be observed that at low damage density conditions, the material integrity increases with the increasing dosage of SBS and TB, indicating that the addition of composite modifiers can effectively enhance the fatigue resistance of the asphalt binder matrix. Furthermore, it is worth noting that for S_2R_{10}, at damage densities greater than 200, the *C* value gradually becomes lower than S_3, approaching that of S_2. This suggests that at higher damage densities, the enhancement of asphalt binder matrix durability by low dosage TB is relatively weak.

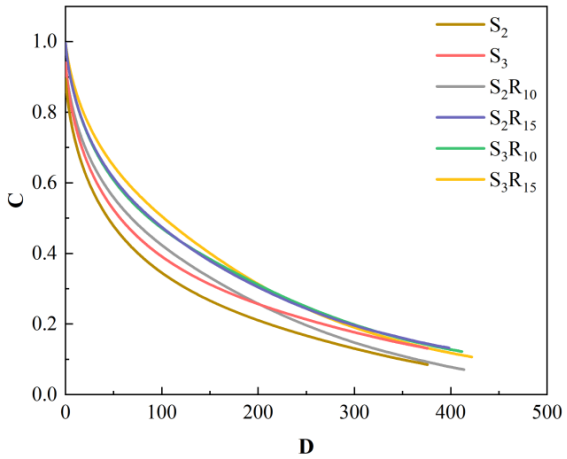

Figure. 7. *D-C* Curves of Samples

Figure 8 shows the predicted fatigue life of various samples calculated using the VECD theory at two strain levels. At a 2.5% strain condition, as the dosage of SBS and TB increases, the fatigue life of the samples gradually increases. The addition of 10% and 15% TB can respectively increase the fatigue life of S_2 by 0.9 times and 5.55 times, and that of S_3 by 1.22 times and 5.77 times. It can also be noted that the fatigue life of S_3 is higher than that of S_2R_{10}, indicating that the enhancement of fatigue resistance in the asphalt binder matrix by low-dosage TB is weaker than that of SBS. Overall, the addition of SBS/TB composite modifiers is beneficial for improving the fatigue resistance of asphalt binder, and this improvement is equally prominent at low and high strain levels.

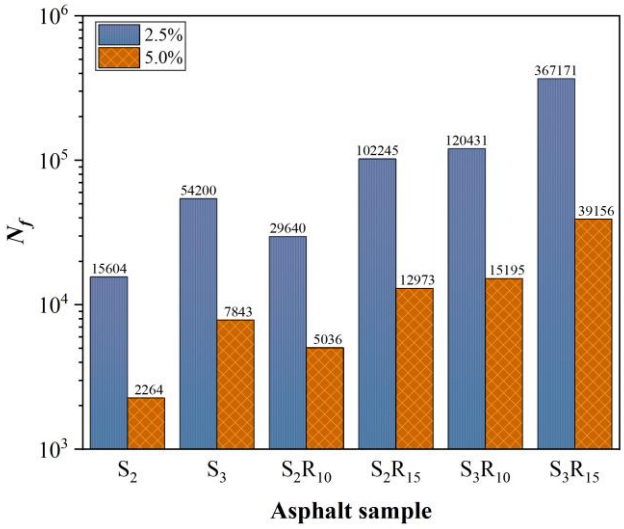

Figure. 8. LAS test results

3.3 DSR-C Fatigue Damage Model Based on TS and LAS Tests

Traditional TS and LAS tests have often been used to define fatigue damage in asphalt binders. However, defining fatigue damage in asphalt binder using fatigue life has indirect and empirical aspects. It cannot explain the mechanisms of fatigue damage in asphalt binder, nor can it reflect the cracking process, or crack propagation, of asphalt binder under rotational shear fatigue loads. To enhance our understanding of fatigue cracks and establish a grading system for asphalt binder fatigue performance, Zhang and Gao, among others, introduced the principles of damage mechanics and proposed a new asphalt binder fatigue performance evaluation model known as the Damage-Based Shear Rheology Crack (DSR-C) model. The DSR-C model utilizes two damage mechanics equilibrium principles, namely the torque balance principle and the Dissipated Strain Energy (DSE) balance principle[30-32] (as shown in Equations 8 and 9). It assumes that the torque and DSE under damaged conditions in asphalt binder are equal to the torque and DSE under undamaged conditions. This model establishes fatigue crack calculation formulas for asphalt binder in two states (undamaged and damaged), based on rheological properties (Equation 10):

$$\frac{\pi r_0^{\ 3}}{2}\tau_{N\max}=\frac{\pi r_E^{\ 3}}{2}\tau_{E\max} \quad (8)$$

$$\int_0^{r_0}\pi\tau_N\left(r\right)^2\frac{\sin\delta_N}{\left|G_N^{\ *}\right|}g2\pi rghgdr=\int_0^{r_E}\pi\tau_E\left(r\right)^2\frac{\sin\delta_0}{\left|G_0^{\ *}\right|}g2\pi rghgdr \quad (9)$$

$$c = \left[1 - \left(\frac{|G_N^*| / \sin(\delta_N)}{|G_0^*| / \sin(\delta_0)}\right)^{\frac{1}{4}}\right] r_0 \quad (10)$$

Where $\tau_{N\max}$ is the maximum stress amplitude of the sample under damage conditions after the nth loading cycle. $\tau_{E\max}$ is the maximum effective stress amplitude of the asphalt binder under undamaged conditions. r_0 is the radius of the fatigue test sample (4 mm). h is the thickness of the fatigue test sample (2 mm). r_E is the effective radius of the sample after the fatigue test, representing the radius of the uncracked area of sample in the DSR test. $|G_0^*|$ and δ_0 are the dynamic modulus and phase angle of the asphalt binder under undamaged conditions. $|G_N^*|$ and δ_N are the dynamic modulus and phase angle of the asphalt binder under the nth loading cycle in time sweep.

This formula ignores the process of how materials transition from an undamaged state to a damaged state. Therefore, the prediction of crack damage only involves material properties in two mechanical states. Compared to the LAS fatigue life prediction model based on Viscoelastic Continuum Damage (VECD) mechanics, this method does not require information about material characteristics during the evolution of damage, such as how the material transitions from a linear viscoelastic state to a nonlinear viscoelastic state and a damaged state. This makes the acquisition and calculation of model parameters more straightforward. The rheological parameters of asphalt binder before and after fatigue damage can be obtained through LAS and TS tests.

3.3.1 Acquisition of Rheological Parameters Before and After Asphalt Binder Fatigue Damage

LAS tests were conducted on various samples to obtain the undamaged shear modulus ($|G_0^*|$) and phase angle (δ_0) at a test temperature of 20°C and a shear loading frequency of 10 Hz. The strain amplitude increased linearly from 0.1% to 30%. During this process, complex modulus and phase angle results for each sample were recorded, and the curves of G^* and δ with shear strain amplitude were plotted (as shown in Figure 9). From the results in the graph, it can be observed that at lower shear strain levels, all samples exhibit a plateau region in both complex modulus and phase angle. As the shear strain increases, the complex modulus gradually decreases, while the phase angle increases, indicating a gradual decline in the rheological properties of the asphalt binders. The undamaged shear modulus ($|G_0^*|$) and phase angle (δ_0) for each asphalt binder were determined by averaging the data from the linear viscoelastic region (plateau stage) in Figure 9. It can be seen that increasing the SBS dosage results in higher modulus and lower phase angle for the asphalt binder, while the impact of TB on the asphalt binder is mainly reflected in an increase in complex modulus, with no clear pattern in phase angle changes.

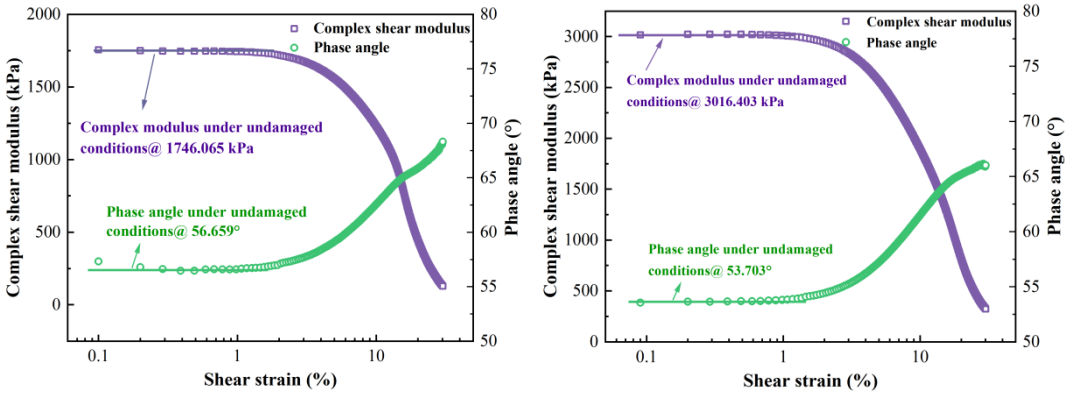

(a) S_2

(b) S_3

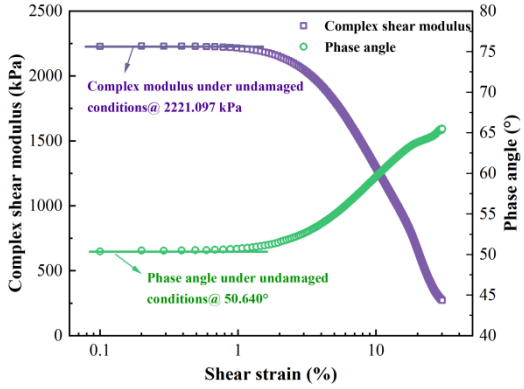

(c) S_2R_{10}

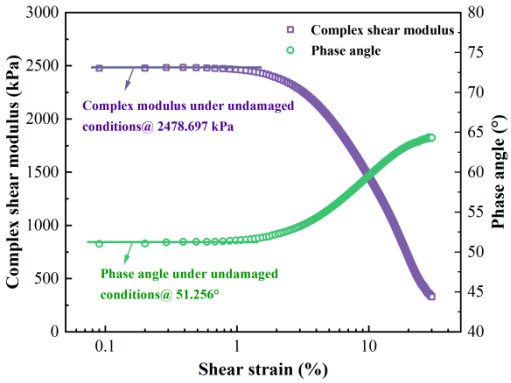

(d) S_2R_{15}

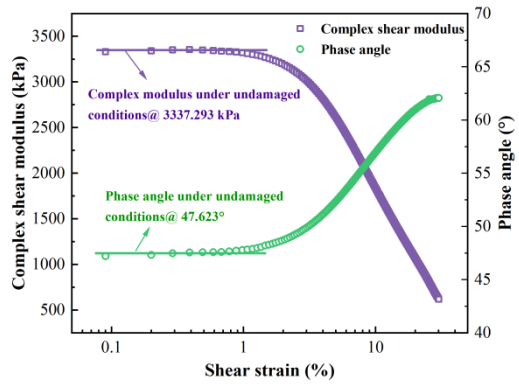

(e) S_3R_{10}

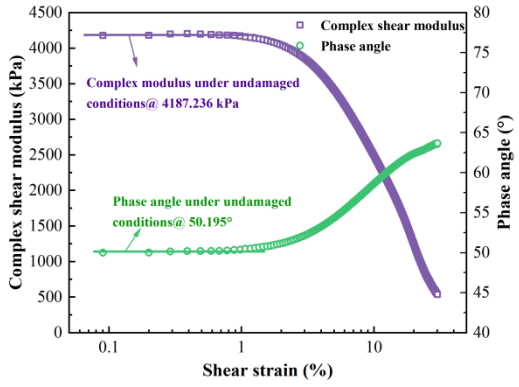

(f) S_3R_{15}

Figure. 9. |G0*| and δ0 results for various samples

The shear modulus ($|G_N^*|$) and phase angle (δ_N) under damaged conditions can be obtained through TS tests. In this study, the test temperature was set at 20°C, and the test frequency was 10 Hz. Based on the LAS test results, when the strain level reached 5%, all samples exhibited significant changes in complex modulus and phase angle. Therefore, a strain level of 5% was selected for the TS test to ensure that the samples would experience noticeable fatigue damage. The number of loading cycles for the TS test was set at 54,000 cycles. The relationship curves between complex modulus and phase angle for each asphalt binder obtained during the TS test are shown in Figure 10. From the graph, it can be seen that the complex modulus of the asphalt binders exhibits a significant decline during loading, while the

phase angle changes relatively little. The complex modulus and phase angle values marked in the graph are the values of $|G_N^*|$ and δ_N when the number of loading cycles reaches 54,000 (N = 54,000).

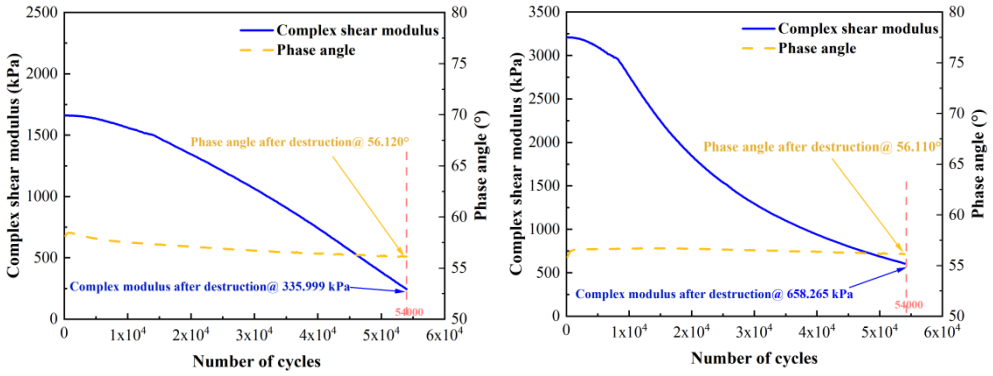

（a）S_2

（b）S_3

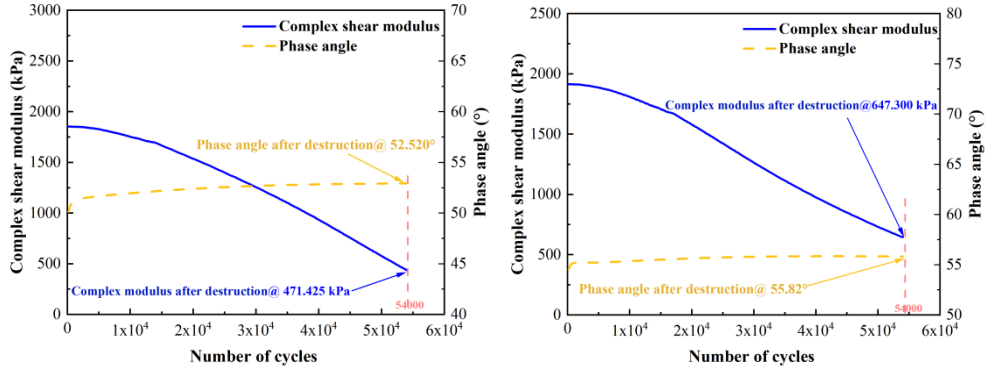

（c）S_2R_{10}

（d）S_2R_{15}

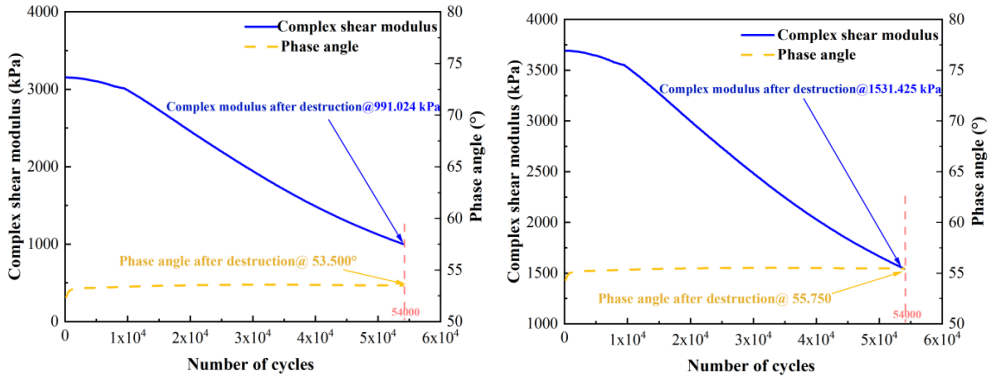

（e）S_3R_{10}

（f）S_3R_{15}

Figure. 10. |GN*| and δ_N results for various samples

3.3.2 Verification of DSR-C Model Fatigue Crack Results

By substituting the obtained $|G_0^*|$, δ_0, $|G_N^*|$, and δ_N results into the DSR-C crack calculation model (Equation 10), the calculated fatigue crack lengths for each asphalt binder can be determined. To further validate the accuracy of the DSR-C model fatigue crack calculation values, an image analysis method was used to measure the actual fatigue cracks on samples after TS fatigue testing. By comparing the calculated values with the measured values, the reliability of the model was verified. The process of measuring fatigue cracks in samples in a damaged state is as follows:

Obtaining Images of Asphalt Binders Surface in Fatigue Damage State: After undergoing 54,000 loading cycles in the TS test, the asphalt binders were subjected to a cooldown to 3°C to prevent asphalt

binders specimen melting and preserve crack morphology and geometry. Then, the top loading rotor was separated from the bottom loading base axially, and the sample was removed from the apparatus. The surface morphology of the samples was photographed at this point, resulting in the original fatigue damage images[30]. The images of typical asphalt binders cracking surfaces obtained from this process are shown in Figure 11. From the images, it can be observed that the samples surface exhibits different forms in different regions. In the central area of the samples, the surface is flat and smooth, representing the undamaged portion of the sample during the time sweep test. In the edge area of the sample, a circular rough surface composed of radial peaks and valleys (referred to as "roof-type cracks") is caused by the interaction between the samples surface and the bottom due to shear loading. The definition of fatigue cracks, as indicated in the graph for S_2, is the difference between the radius r_0 of the asphalt binder test sample and the effective radius r_E, which represents the radius of the uncracked area of the sample in the DSR test.

Figure. 11. Images of asphalt binders fatigue cracking surfaces under loading conditions of 20 ℃ and 10 Hz (54,000 loading cycles)

Measurement of Actual Fatigue Cracks: Firstly, the original damage images were processed, and specific areas involved in the process were defined (as illustrated for S_2 in Figure 12). Based on significant differences in grayscale values, the boundaries between undamaged and cracked areas were marked using Adobe Photoshop CS6 software. Then, pixel area statistics functions in Image Pro Plus (IPP) 6.0 software were used to calculate the pixel area of the undamaged area and the entire sample area, and the pixel area ratio (S_e/S_0) was used to replace the actual area ratio. Finally, the crack length (c), represented as the measured crack length, was obtained using Equation 11:

$$c = \frac{d_0\left(1-\sqrt{S_e / S_0}\right)}{2} \quad (11)$$

Where d_0 is the diameter of the sample, which is 8 mm.

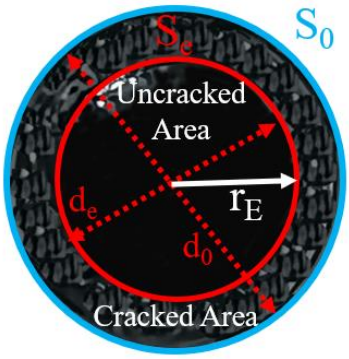

Figure. 12. Schematic diagram of fatigue crack measurement for S_2 samples

Based on the above process, calculated fatigue crack lengths and model calculation values were obtained for each asphalt binder using the DSR-C model. Additionally, to ensure the accuracy of the model validation results and discuss the impact of the number of loading cycles on the model accuracy, the same method was used to calculate fatigue crack values and measurements for 42,000 loading cycles for each asphalt binder. The results for both loading cycle conditions are shown in Tables 6 and 7. Comparing the two tables, it is evident that the fatigue crack length values for asphalt binder under 54,000 loading cycles are larger, indicating that an increase in the number of loading cycles exacerbates the fatigue damage in the asphalt binder. Additionally, it is apparent that the addition of SBS and TB improves the asphalt binder resistance to fatigue damage. The fatigue performance ranking of the various asphalt binders is consistent for both loading cycle conditions, indicating that the asphalt binders resistance to fatigue performance is in the following order: $S_3R_{15} > S_3R_{10} > S_2R_{15} > S_3 > S_2R_{10} > S_2$. Based on the results of fatigue crack lengths, it can be concluded that the combination of 3% SBS and 15% TB is more effective in inhibiting fatigue cracking in asphalt binders.

The correlation analysis results between the DSR-C model fatigue crack calculation values and the measured values for different loading cycles are shown in Figure 13. It can be observed that the calculated crack values and measured values for all seven asphalt binders exhibit a good correlation. Furthermore, under 54,000 loading cycles, there is a higher correlation between the crack length calculation values and the measured values, indicating that the model accuracy improves with an increase in the number of shear loading cycles, making the model more advantageous for characterizing asphalt binders with greater degrees of fatigue damage.

Table 6 Model parameters and crack results for asphalt binders under 42,000 loading cycles

Asphalt Binder	G_0^* (kPa)	δ_0 (°)	G_N^* (kPa)	δ_N (°)	Model Calculation (mm)	Measured (mm)
S_2	1746.065	56.659	416.759	55.271	1.193	1.279
S_3	3016.403	53.703	835.265	55.213	1.112	1.083
S_2R_{10}	2221.097	50.640	567.561	51.833	1.168	1.259
S_2R_{15}	2478.697	51.256	859.293	54.620	0.964	1.026
S_3R_{10}	3337.293	47.623	1286.172	51.511	0.894	0.948
S_3R_{15}	4187.236	50.195	1656.825	53.782	0.866	0.924

Table 7 Model parameters and crack results for asphalt binders under 54,000 loading cycles

Asphalt Binder	G_0^* (kPa)	δ_0 (°)	G_N^* (kPa)	δ_N (°)	Model Calculation (mm)	Measured (mm)
S_2	1746.065	56.659	335.999	56.120	1.347	1.306

S_3	3016.403	53.703	658.265	56.112	1.286	1.259
S_2R_{10}	2221.097	50.640	471.425	52.523	1.303	1.325
S_2R_{15}	2478.697	51.256	647.300	55.822	1.182	1.169
S_3R_{10}	3337.293	47.623	991.024	53.517	1.109	1.038
S_3R_{15}	4187.236	50.195	1531.425	55.751	0.946	0.909

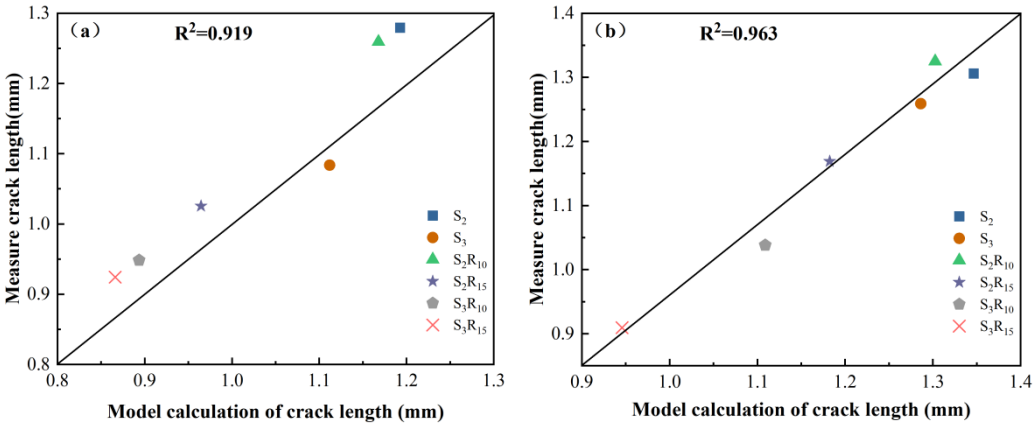

Figure. 13. Correlation between DSR-C model fatigue crack calculation values and measured values: (a) 42,000 loading cycles; (b) 54,000 loading cycles

3.4 Comparison of Fatigue Damage Evaluation Models for SBS/TB Composite Modified Asphalt Binder

To intuitively compare the accuracy of different asphalt binders fatigue damage assessment models, this study uses Taylor diagrams to comprehensively compare the *R*, centered root mean square error (CRMS), and standard deviation (σ) among traditional TS and LAS test related evaluation models. This analysis aims to identify a more suitable fatigue damage assessment model for SBS/TB composite modified asphalt binder.

The Taylor diagram is a representation method first proposed by Karl E. Taylor in 2001, which succinctly summarizes the correspondence between simulated and observed fields[33]. It is essentially based on the cosine relationship formed by the correlation coefficient, root mean square difference, and standard deviation. These three correlation evaluation indicators are integrated into a polar plot. In this plot, the correlation coefficient, root mean square difference, and the ratio of standard deviations between the two models are represented by a single point in a two-dimensional (2-D) graph. This allows for the assessment of the accuracy of different models in simulating real situations. The Taylor diagram has significant advantages in assessing the relative merits of competing models and overall performance monitoring as models evolve.

The R, CRMS, σ between models can be calculated using the following equations:

$$R = \frac{\frac{1}{N}\sum_{n=1}^{N}(f_n - \overline{f})(r_n - \overline{r})}{\sigma_f \sigma_r} \quad (12)$$

$$CRMS = \left\{\frac{1}{N}\sum_{n=1}^{N}\left[(f_n - \overline{f}) - (r_n - \overline{r})\right]^2\right\}^{1/2} \quad (13)$$

$$\sigma = \left[\frac{1}{N}\sum_{n=1}^{N}(A_n - \overline{A})^2\right]^{1/2} \quad (14)$$

Where r represents the actual measurement values, f and A represent model calculated values.

Based on the results of Section 3.3.2, the DSR-C fatigue assessment model calculated crack length has a good correlation with the observed fatigue crack length in samples. Therefore, this study selects the DSR-C model as the "benchmark" model. Based on the results of Sections 3.1 and 3.2, the phase angle peak criterion of the TS test is not suitable for evaluating the fatigue performance of SBS/TB modified asphalt binder. Therefore, this model is not included in the comparison. Additionally, since the TS test results are all obtained at a 5% strain level, to ensure consistency in external conditions for model comparison, the fatigue life results calculated by the VECD model at a 2.5% strain level are also not included in the comparison. In summary, the models participating in the comparison are the complex modulus decay criterion model (50%G^*), S×N peak criterion model, 20%DER deviation criterion model, and VECD model (5% strain).

However, the parameters compared in the Taylor diagram should have consistency. The evaluation indicator of the DSR-C model (fatigue crack length) is not on the same scale as the evaluation indicators of other models (fatigue life). Therefore, it is necessary to convert the fatigue crack length of the DSR-C model into fatigue life. According to the research by Zhang, Gao, and others, asphalt binder crack propagation can be divided into three stages: the initial transition period (Stage I), stable growth period (Stage II), and rapid growth period (Stage III). Among them, when the crack length reaches the critical point of the separation load cycles, it enters the rapid crack growth stage (Stage III). This separation load cycle (critical point of Stages II and III) can be considered as the fatigue life N_f of the asphalt binder. According to this theory, the DSR-C model is used to calculate the fatigue crack length of asphalt binders under different loading cycles, and the crack propagation curve during fatigue loading is plotted. As shown in Figure 14, taking S_2 and S_3 as examples, the fatigue crack propagation of asphalt binders conforms to the three-stage theory. Thus, the fatigue life values based on the DSR-C model can be calculated for various samples.

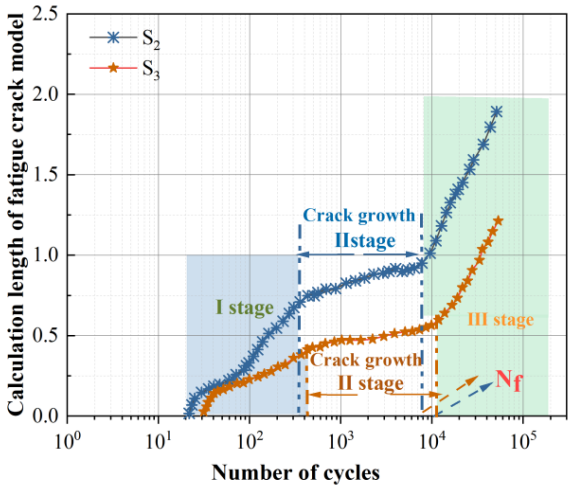

Figure. 14. Asphalt binders Fatigue Crack Propagation Curve

The calculated fatigue life results for various samples obtained from each model are shown in Table 8, and the Taylor diagrams of simulated fatigue life by each model are shown in Figure 15.

In Figure 15, the fatigue life results calculated by the DSR-C model are the reference values (REF), and the calculated values of the other four models closer to the DSR-C model (in red) indicate better fitting of fatigue life by those models. Overall, the 20%DER deviation criterion model and VECD model are close in their comprehensive simulation results, with better simulation results for standard deviation

and RMSE but slightly lower correlation coefficients. For the other models, the 50%G* criterion model has a better fit for the correlation coefficient, which is 0.9289, but it has larger standard deviation and RMSE. The S×N peak criterion model has a better fit for the correlation coefficient but a poorer fit for the standard deviation.

To more accurately assess the comprehensive simulation accuracy of each model, T_S are introduced to compare the fitting results of each model, defined as in equation (15).

$$T_S = 4(1+r)^4 / [\,(\frac{STD_m}{STD_0} + \frac{STD_0}{STD_m})^2 (1+r_o)^4\,] \quad (15)$$

Where r represents the correlation coefficient between each model and REF, r_0 is the maximum value of r, STD_m is the standard deviation of each model, STD_0 is the standard deviation of REF, and TS values range from 0 to 1. A higher T_S value indicates better simulation results. The T_S results for each model are shown in Table 9. It can be concluded that the 20%DER deviation criterion model performs the best in terms of comprehensive simulation results, followed by VECD model, while the 50%G* and S×N peak criterion models have lower T_S. These results suggest that DSR-C model, 20%DER deviation criterion, and VECD model are more suitable as fatigue damage assessment models for SBS/TB composite modified asphalt binder, whereas traditional evaluation criteria based on TS tests have lower accuracy.

Table 8 Fatigue Life Calculation Results of Various Fatigue Models for Asphalt Binders

Model	N_f					
	S_2	S_3	S_2R_{10}	S_2R_{15}	S_3R_{10}	S_3R_{15}
DSR-C (REF)	7783	11892	9753	22670	31234	38562
50%G*	7020	28200	24180	33780	41820	60180
S×N Peak Criterion	8375	21348	24268	24583	32480	42657
20%DER Deviation Criterion	5162	10257	8435	12346	22460	25470
VECD	2264	7843	5036	12973	15195	39156

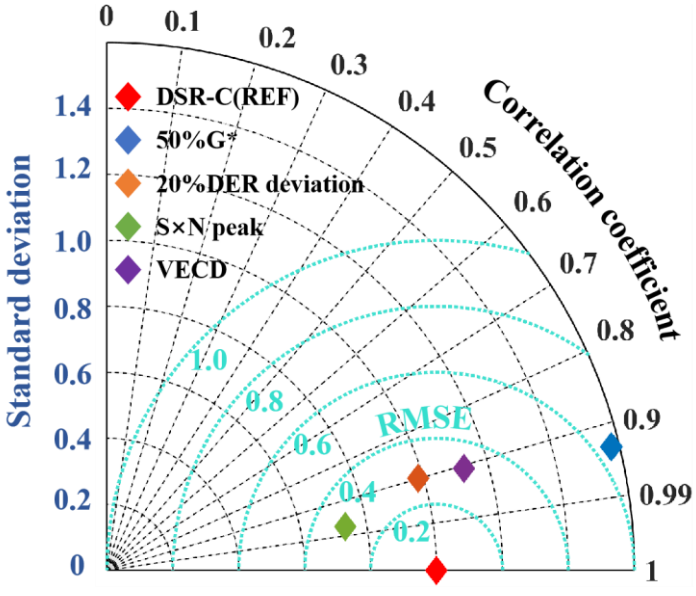

Figure. 15. Taylor Diagrams of Simulated Fatigue Life by Different Fatigue Damage Models

Table 9 T_S Scores of Various Fatigue Models for Asphalt Binders Fatigue Life Assessment

Fatigue Model	50%G^*	S×N Peak Criterion	20%DER Deviation Criterion	VECD
T_S	0.8289	0.8197	0.8792	0.8639

4 Conclusion

This study comprehensively evaluated the fatigue performance of SBS/TB composite modified asphalt binder using the fatigue failure criteria of TS tests, LAS tests based on the VECD model, and the DSR-C fatigue crack model. The predictive fatigue results of the DSR-C model were verified using image analysis. Taylor diagrams were used to compare and analyze the simulation accuracy of various fatigue damage evaluation models. The main conclusions are as follows:

(1) The TS test results suggest that the addition of TB effectively delays the fatigue failure of SBS asphalt binder. However, it is noted that the phase angle peak criterion of the TS test is not the most suitable metric for evaluating the fatigue performance of SBS/TB composite modified asphalt binder.

(2) LAS test findings underscore the significant improvement in fatigue resistance of asphalt binder due to composite modifiers across various strain levels. Notably, TB enhances fatigue resistance by widening the range of yield stress peak in asphalt and reducing both stress peaks and strain dependency.

(3) The fatigue crack length index derived from the DSR-C model provides a more intuitive and precise depiction of cracking progression in SBS/TB composite modified asphalt binder under fatigue loads. Furthermore, it exhibits a robust correlation with actual fatigue cracking observed in asphalt binder.

(4) Taylor diagram results for fatigue life, utilizing various fatigue damage models, indicate that the DSR-C model, the 20% DER deviation criterion, and the VECD model are more suitable as fatigue damage evaluation models for SBS/TB composite modified asphalt binder.

In future studies, we aim to further explore the applicability of the DSR-C model to other modified asphalts. Additionally, we plan to compare fatigue assessment methods of other asphalt types using both the Taylor diagram and TS test, striving to identify a fatigue assessment method that is universally suitable for various modified asphalts, enhancing the comprehensiveness of our findings and aligning with similar investigations.

Credit Author Statement

Huikun Chen: Data curation, Writing-original draft. **Shan Huang**: Data curation, Writing-original draft. **Dongyu Niu**: Supervision, Methodology, Writing - review & editing. **Yangming Gao**: Supervision, Writing - review & editing. **Zhao Zhang**: Investigation, Methodology.

Declaration of Competing Interest

The authors declare that they have no known competing financial interests or personal relationships that could have appeared to influence the work reported in this paper.

Acknowledgements

This work was supported by the Natural Science Basic Research Program of Shaanxi (2024JC-YBMS-374), the project of Zhengcheng R&D Center (ZCYF-2023-01-01).

References

[1] L. Haibin, Z. Yongfei, Z. Mingming, C. Canyang, H. Gongxin, Z. Lichang, Optimizing parameters for the preparation of low viscosity rubber asphalt incorporating waste engine oil using response surface methodology, Environmental Science and Pollution Research (2023). https://doi.org/10.1007/s11356-023-28383-2

[2] Y. Meng, X. Ye, F. He, Z. Chen, C. Hu, P. Lin, Comprehensive study on the degradation progress of crumb tire rubber during the preparation of terminal blended rubberized asphalt binder, Journal of Cleaner Production 417 (2023) 137916. https://doi.org/10.1016/j.jclepro.2023.137916

[3] J. Xie, X. Zhao, S. Lv, Y. Zhang, W. He, F. Yu, Research on performance and mechanism of terminal blend/grafting activated crumb rubber composite modified asphalt, Construction and Building Materials 394 (2023) 132225. https://doi.org/10.1016/j.conbuildmat.2023.132225

[4] J. Zhang, W. Huang, Y. Zhang, C. Yan, Q. Lv, W. Guan, Evaluation of the terminal blend crumb rubber/SBS composite modified asphalt, Construction and Building Materials 278 (2021) 122377. https://doi.org/10.1016/j.conbuildmat.2021.122377

[5] N. Tang, C. Xue, G. Hao, W. Huang, H.-m. Zhu, R. Li, Sustainable production of eco-friendly rubberized asphalt binders through chemically crosslinking with polymer modifier, Journal of Cleaner Production (2023). https://doi.org/10.1016/j.jclepro.2023.138633

[6] H. Nan, Y. Sun, J. Chen, M. Gong, Investigation of fatigue performance of asphalt binders containing SBS and CR through TS and LAS tests, Construction and Building Materials 361 (2022) 129651. https://doi.org/10.1016/j.conbuildmat.2022.129651

[7] Y. Gao, Y. Zhang, Y. Yang, J. Zhang, F. Gu, Molecular dynamics investigation of interfacial adhesion between oxidised bitumen and mineral surfaces, Applied Surface Science 479 (2019) 449-462. https://doi.org/10.1016/j.apsusc.2019.02.121

[8] Y. Zhang, X. Luo, R. Luo, R.L. Lytton, Crack initiation in asphalt mixtures under external compressive loads, Construction and Building Materials 72 (2014) 94-103. https://doi.org/10.1016/j.conbuildmat.2014.09.009

[9] J.P. Planche, D.A. Anderson, G. Gauthier, Y.M. Le Hir, D. Martin, Evaluation of fatigue properties of bituminous binders, Materials and Structures 37(269) (2004) 356-359. https://doi.org/10.1617/14127

[10] B.W. Tsai, C.L. Monismith, Aapt, Influence of asphalt binder properties on the fatigue performance of asphalt concrete pavements, 2005 Journal of The Association of Asphalt Paving Technologists: From the Proceedings of The Technical Sessions, Vol 74, 2005, pp. 733-789.

[11] F.J. Zhou, W. Mogawer, H.S. Li, A. Andriescu, A. Copeland, Evaluation of Fatigue Tests for Characterizing Asphalt Binders, Journal of Materials in Civil Engineering 25(5) (2013) 610-617. https://doi.org/10.1061/(ASCE)MT.1943-5533.0000625

[12] H.U. Bahia, H.C. Zhai, M.L. Zeng, Y. Hu, P. Turner, Aapt, Aapt, Aapt, Development of binder specification parameters based on characterization of damage behavior, Journal of the Association of Asphalt Paving Technologists, Vol 70: Asphalt Paving Technology 2001, 2001, pp. 442-470.

[13] D.A. Anderson, Y.M. Le Hir, M.O. Marasteanu, J.P. Planche, D. Martin, G. Gauthier, Nrc,

Nrc, Evaluation of fatigue criteria for asphalt binders, Asphalt Binders 2001: Materials and Construction2001, pp. 48-56. http://worldcat.org/isbn/309072271

[14] K.S. Bonnetti, K. Nam, H.U. Bahia, Trb, Trb, Measuring and defining fatigue behavior of asphalt binders, Bituminous Binders 2002: Materials and Construction2002, Pp. 33-43. http://worldcat.org/isbn/0309077362

[15] C. Wang, H. Zhang, C. Castorena, J.X. Zhang, Y.R. Kim, Identifying fatigue failure in asphalt binder time sweep tests, Construction and Building Materials 121 (2016) 535-546. https://doi.org/10.1016/j.conbuildmat.2016.06.020

[16] K.A. Ghuzlan, S.H. Carpenter, Trb, Trb, Trb, Trb, Energy-derived, damage-based failure criterion for fatigue testing, 2000 Trb Distinguished Lecture, Pt 1 - Asphalt Mixtures 2000, Pt 2: Materials and Construction2000, pp. 141-149.

[17] S.H. Carpenter, S. Shen, Trb, Dissipated energy approach to study hot-mix asphalt healing in fatigue, Bituminous Paving Mixtures 2006, 2006, pp. 178-+. https://doi.org/10.1177/0361198106197000119

[18] S.H. Shen, S.H. Carpenter, Trb, Application of the dissipated energy concept in fatigue endurance limit testing, Bituminous Paving Mixtures 2005, pp. 165-173. https://doi.org/10.3141/1929-20

[19] S.H. Shen, H.M. Chiu, H. Huang, Characterization of Fatigue and Healing in Asphalt Binders, Journal of Materials in Civil Engineering 22(9) (2010) 846-852. https://doi.org/10.1061/(ASCE)MT.1943-5533.0000080

[20] B. Asadi, N. Tabatabaee, R. Hajj, Use of linear amplitude sweep test as a damage tolerance or fracture test to determine the optimum content of asphalt rejuvenator, Construction and Building Materials 300 (2021) 123983. https://doi.org/10.1016/j.conbuildmat.2021.123983

[21] I. Binti Joohari, F. Giustozzi, Oscillatory shear rheometry of hybrid polymer-modified bitumen using multiple stress creep and recovery and linear amplitude sweep tests, Construction and Building Materials 315 (2022) 125791. https://doi.org/10.1016/j.conbuildmat.2021.125791

[22] C. Hintz, H. Bahia, Understanding mechanisms leading to asphalt binder fatigue in the dynamic shear rheometer, Road Materials and Pavement Design 14 (2013) 231-251. https://doi.org/10.1080/14680629.2013.818818

[23] L.Y. Shan, S. Tian, H.S. He, N.Q. Ren, Internal crack growth of asphalt binders during shear fatigue process, FUEL 189 (2017) 293-300. https://doi.org/10.1016/j.fuel.2016.10.094

[24] S.W. Park, Y.R. Kim, R.A. Schapery, A viscoelastic continuum damage model and its application to uniaxial behavior of asphalt concrete, Mechanics of Materials 24(4) (1996) 241-255. https://doi.org/10.1016/s0167-6636(96)00042-7

[25] C.Q. Yan, L.X. Yuan, X.T. Yu, S.Z. Ji, Z.F. Zhou, Characterizing the fatigue resistance of multiple modified asphalts using time sweep test, LAS test and elastic recovery test, Construction and Building Materials 322 (2022). https://doi.org/10.1016/j.conbuildmat.2021.125806

[26] H. Chen, Y. Zhang, H.U. Bahia, The Role of Binders in Cracking Resistance of Mixtures Measured with The IFIT Procedure, The 64th Annual Meeting of the Canadian Technical Asphalt Association, 2019.

[27] H. Chen, H.U. Bahia, Modelling effects of aging on asphalt binder fatigue using complex modulus and the LAS test, International Journal of Fatigue 146 (2021).

https://doi.org/10.1016/j.ijfatigue.2021.106150

[28] S. Zhao, B.S. Huang, X. Shu, J. Moore, B. Bowers, Effects of WMA Technologies on Asphalt Binder Blending, Journal of Materials in Civil Engineering 28(2) (2016). https://doi.org/10.1061/(ASCE)MT.1943-5533.0001381

[29] Y.Q. Bi, S.F. Wu, J.Z. Pei, Y. Wen, R. Li, Correlation analysis between aging behavior and rheological indices of asphalt binder, Construction and Building Materials 264 (2020). https://doi.org/10.1016/j.conbuildmat.2020.120176

[30] Y.Q. Zhang, Y.M. Gao, Predicting crack growth in viscoelastic bitumen under a rotational shear fatigue load, ROAD Materials and Pavement Design 22(3) (2021) 603-622. https://doi.org/10.1080/14680629.2019.1635516

[31] Y.M. Gao, L.L. Li, Y.Q. Zhang, Modeling Crack Propagation in Bituminous Binders under a Rotational Shear Fatigue Load using Pseudo J-Integral Paris' Law, Transportation Research Record 2674(1) (2020) 94-103. https://doi.org/10.1177/0361198119899151

[32] Y.M. Gao, L.L. Li, Y.Q. Zhang, Modelling crack initiation in bituminous binders under a rotational shear fatigue load, International Journal of Fatigue 139 (2020). https://doi.org/10.1016/j.ijfatigue.2020.105738

[33] Taylor, E. Karl, Summarizing multiple aspects of model performance in a single diagram, Journal of Geophysical Research Atmospheres 106(D7) (2001) 7183-7192. https://doi.org/10.1029/2000JD900719